Ivan T. Demchenko, Karen E. Welty-Wolf, Barry W. Allen and Claude A. Piantadosi

You might find this additional information useful...

This article cites 56 articles, 26 of which you can access free at:
http://ajplung.physiology.org/cgi/content/full/293/1/L229#BIBL

Updated information and services including high-resolution figures, can be found at:
http://ajplung.physiology.org/cgi/content/full/293/1/L229

Additional material and information about *AJP - Lung Cellular and Molecular Physiology* can be found at:

http://www.the-aps.org/publications/ajplung

This information is current as of September 16, 2007 .

Similar but not the same: normobaric and hyperbaric pulmonary oxygen toxicity, the role of nitric oxide

Ivan T. Demchenko,[1,2,4] Karen E. Welty-Wolf,[1,3] Barry W. Allen,[1,2] and Claude A. Piantadosi[1,2,3]

[1]*Center for Hyperbaric Medicine and Environmental Physiology,* [2]*Department of Anesthesiology, and* [3]*Division of Pulmonary Medicine, Department of Medicine, Duke University Medical Center, Durham, North Carolina; and* [4]*Institute of Evolutionary Physiology and Biochemistry, Russian Academy of Sciences, St. Petersburg, Russia*

Demchenko IT, Welty-Wolf KE, Allen BW, Piantadosi CA. Similar but not the same: normobaric and hyperbaric pulmonary oxygen toxicity, the role of nitric oxide. *Am J Physiol Lung Cell Mol Physiol* 293: L229–L238, 2007. First published April 6, 2007; doi:10.1152/ajplung.00450.2006.—Pulmonary manifestations of oxygen toxicity were studied and quantified in rats breathing >98% O_2 at 1, 1.5, 2, 2.5, and 3 ATA to test our hypothesis that different patterns of pulmonary injury would emerge, reflecting a role for central nervous system (CNS) excitation by hyperbaric oxygen. At 1.5 atmosphere absolute (ATA) and below, the well-recognized pattern of diffuse pulmonary damage developed slowly with an extensive inflammatory response and destruction of the alveolar-capillary barrier leading to edema, impaired gas exchange, respiratory failure, and death; the severity of these effects increased with time over the 56-h period of observation. At higher inspired O_2 pressures, 2–3 ATA, pulmonary injury was greatly accelerated but less inflammatory in character, and events in the brain were a prelude to a distinct lung pathology. The CNS-mediated component of this lung injury could be attenuated by selective inhibition of neuronal nitric oxide synthase (nNOS) or by unilateral transection of the vagus nerve. We propose that extrapulmonary, neurogenic events predominate in the pathogenesis of acute pulmonary oxygen toxicity in hyperbaric oxygenation, as nNOS activity drives lung injury by modulating the output of central autonomic pathways.

central nervous system oxygen toxicity; hyperbaric oxygen

THE MAMMALIAN LUNG IS A PRIMARY target of the toxic effects of oxygen, however, at high oxygen partial pressures, acute manifestations of toxicity appear in the brain, including electrical discharges on the electroencephacogram, resulting in muscular jerks and convulsions. The central nervous system (CNS) effects appear relatively rapidly when inspired oxygen exceeds 2.0 atmosphere absolute (ATA), as reviewed by Balentine in 1982 (2) and Clark and Thom in 2003 (11). In normobaric conditions, direct pulmonary injury predominates, and relatively long exposures at inspired oxygen pressures ranging from 0.6 to 1.0 ATA cause diffuse damage to both alveolar epithelium and pulmonary capillary endothelium, resulting in interstitial and intra-alveolar edema, impaired gas exchange, and extensive infiltration by inflammatory cells (2, 3, 10, 12, 60). For example, adult rats continuously exposed to 100% O_2 at 1 ATA begin to die of respiratory failure within 72 h (13, 14).

Hyperbaric oxygen (HBO$_2$) at 2–4 ATA accelerates the development of gross and histological changes in the lungs, including pulmonary edema, congestion, and intra-alveolar hemorrhage (11), and pulmonary injury is more pronounced in animals that also exhibit the seizures of CNS O_2 toxicity (2, 3). The mechanisms for this neurogenic accentuation of hyperoxic lung injury are unknown.

In normobaric hyperoxia, pulmonary injury has been attributed to the formation of reactive oxygen species (ROS) that overwhelm antioxidant defenses and oxidize lipids, nucleic acids, and proteins in lung tissue (26, 32, 37). The lung is uniquely vulnerable because it presents to the atmosphere a delicate, extensive region, which is the major interface between the external environment and the interior physiological milieu, and it is the only organ through which the total cardiac output must pass.

Since 1991, work in our laboratory has led to the development of the paradigm that O_2-dependent changes in the activity of nitric oxide (NO) in the brain alter susceptibility to CNS O_2 toxicity (45, 61). This hypothesis has been supported by experimental data showing that inhibition of nitric oxide synthase (NOS) prevents or attenuates HBO$_2$-induced seizures (8, 9, 19, 20, 45) and that an increase in cerebral NO production always precedes the onset of O_2 convulsions (18, 20, 21, 28, 51). The observations that HBO$_2$ stimulates NO production in the brain and also accelerates lung damage suggest the hypothesis that NO pathways contribute to the severity of hyperbaric pulmonary oxygen toxicity.

Among the many investigations of pulmonary injury due to normobaric and hyperbaric oxygen, no single study has evaluated the pathological effects of both regimes of hyperoxia, side-by-side and under uniform experimental conditions. Therefore, the work reported here was designed to compare lung injury induced by oxygen under normobaric conditions with that occurring in hyperbaric conditions and to examine the contribution of NO to the acute pulmonary toxicity of hyperbaric hyperoxia.

MATERIALS AND METHODS

Animals and O_2 exposures. Adult male Sprague-Dawley rats (Charles River Laboratories) weighing 283 ± 11 g were used in an experimental protocol approved by the Duke University Institutional Animal Care and Use Committee.

For normobaric experiments, rats were placed in a sealed acrylic chamber and continuously exposed to O_2 with free access to food and water. The O_2 concentration was monitored continuously (model 570 O_2 analyzer, Servomex) and kept at or above 98%. The gas flow through the chamber was ∼12 l/min, sufficient to allow complete gas exchange every 5 min and keep CO_2 levels below that in room air (∼0.5%). The temperature in the chamber was maintained between 22–24°C, and relative humidity between 60–70%.

Hyperbaric experiments were conducted either in a small hyperbaric chamber (Bethlehem, Bethlehem, PA) or in a glove-bag apparatus inside a large pressure chamber (Duke Center for Hyperbaric Medicine and Environmental Physiology). The inspired oxygen concentration was maintained >99%, and CO$_2$ was limited to 0.1%. The temperature in the chamber was maintained between 22–24°C with relative humidity ~60%. Animals were continuously observed, particularly for signs of CNS O$_2$ toxicity.

Experimental design. In the first stage of experimentation, five groups of animals ($n = 10$–12, each group) were exposed to O$_2$ at 1, 1.5, 2, 2.5, or 3 ATA, and survival curves and 50% mortality (LD$_{50}$) were calculated for each exposure. In a second series of experiments, rats were exposed to O$_2$ at the same five pressures for times corresponding to ~80% of the LD$_{50}$ to assess histological and biochemical lung injury and keep mortality below 5%. Two rats were exposed to hyperbaric normoxia (7% O$_2$, 93% N$_2$) at 3 ATA for 6 h as controls to determine if there is any contribution of pressure per se to pulmonary injury. Two additional groups of rats ($n = 8$, each group) were exposed to oxygen at 1 ATA for 24 or 48 h to determine the time dependency of normobaric pulmonary oxygen toxicity. Two more groups ($n = 9$, each group) were used to evaluate the contribution of NO to HBO$_2$-induced lung injury. For this, rats were treated with either 7-nitroindazole (7-NI; 50 mg/kg ip), a selective inhibitor of neuronal NOS (nNOS), or with L-NAME (30 mg/kg ip), a nonselective NOS inhibitor, 30 min before hyperbaric exposure to O$_2$ at 3 ATA for 6 h. Finally, in one more group of rats ($n = 13$), the vagus nerve was unilaterally transected at the cervical level 1 wk before a 6-h exposure to O$_2$ at 3 ATA to assess the effect of partial disruption of neuronal communication between brain and lung on the severity of lung injury.

Tissue collection and lung lavage. Immediately after hyperoxic exposure, each rat was killed with an overdose of halothane, chest and peritoneal cavities were opened carefully, and the volume of pleural fluid was measured by syringe. The right lung was removed and used to assess edema. The remaining lung was prepared for pathology studies as described below. In other rats, tracheotomy was performed, and a 20-gauge × 32-mm needle was inserted and secured for bilateral bronchoalveolar lavage (BAL) with one 10-ml aliquot of sterile, nonpyrogenic phosphate-buffered saline solution. [In some animals that were vagotomized, the contralateral bronchus was clamped, and BAL fluid (BALF) was withdrawn from the ipsilateral lung only, as described below]. The recovered BALF was analyzed for markers of lung injury.

Lung microscopy. Lung tissue was examined by both light and electron microscopy (EM). After removal of the right lung, the left lung was inflation-fixed via the trachea for 15 min at 20 cmH$_2$O fixative pressure with 2% glutaraldehyde in 0.85 M sodium cacodylate buffer (pH 7.4) and then excised and immersed in the same fixative mixture for 24 h. For light microscopy, tissue samples were embedded in paraffin, sectioned, and stained with hematoxylin and eosin. Semiquantitative analysis was performed by a blinded observer on light microscopy sections from animals exposed to 1.0 (60 h), 1.5 (20 h), 2.0 (10 h), and 2.5 (8 h) ATA oxygen as well as to 7% O$_2$ at 3 ATA. Slides from six animals in each group were graded for both extent and severity of injury in three categories of lung pathology: alveolar edema, interstitial and septal thickening, and intra-alveolar cells and debris. For grading the extent of injury, each category was assigned a score of 0 (absent), 1 (<25% involved), 2 (25–50%), 3 (50–75%), or 4 (>75%). For severity, each category was graded at the most involved site as 0 (absent), 1 (mild), 2 (moderate), and 3 (severe). A composite grade for each category was expressed as the product of extent and severity. The total lung injury score for each animal is the sum of the composite grades for each of the three categories.

For EM, tissue cubes were cut from four peripheral sites, washed in cacodylate buffer, and stained with 2% osmium tetroxide. After dehydration in graded ethanol solutions, the tissue was immersed in propylene oxide and embedded in Epon epoxy resin. Thin sections were cut with a diamond knife, placed on coated 200-mesh Cu/Rh grids, and stained with uranyl acetate and lead citrate. Sections were viewed and photographed using a JEOL 100S electron microscope, and the resulting images were enlarged to 8,500× on 11 × 14-in. photographic paper for visual analysis.

Lung edema assessment. As an index of edema, wet-dry weight ratio was assessed in freshly excised lungs. The lungs were weighed immediately on tared foil squares to determine wet weight and then placed in a vacuum oven at 60°F for at least 96 h or until a stable dry weight was obtained. No corrections were made for intravascular lung water.

BALF assay. Total cell counts (cells per milliliter of BALF) were made with a hemocytometer (Neubauer). After centrifugation (3,500 *g* for 5 min at 4°C), lactate dehydrogenase (LDH) activity and total protein content were measured in the supernatant. Total protein includes both plasma proteins and intracellular proteins and indicates damage to the blood-air barrier. The catalytic activity of LDH in cell-free BALF was measured by the amount of L-lactate oxidized at 30°C, per unit time, from reduction of NAD$^+$. Total protein content was measured with the bicinchoninic acid assay using bovine serum albumin as a standard (55).

Measurement of NO and peroxynitrite in BALF. The oxidation products of NO, nitrite and nitrate (NO$_x$), were determined by fluorometric assay (43, 44). Briefly, to convert nitrate to nitrite, deproteinized BALF (200 µl) was incubated with 10 µl of nitrate reductase (5 U/ml, Sigma) in the presence of 10 µl of FAD and 10 µl of NADPH. Then, excess NADPH was oxidized with 2 U/ml LDH. The samples were reacted in the dark for 10 min with 25 µl of 2,3-diaminonaphthalene (DAN) at room temperature. The pH of the mixture was adjusted to 11.5–12 with 1 N NaOH, and fluorescence was measured using a 96-well plate fluorescence spectrophotometer (Safire; Teca, Durham, NC). Nitrite concentration in the sample was calculated from the linear region (0.02–3.2 µM) of a standard curve constructed using sodium nitrite standards (Sigma) diluted in 0.9% NaCl.

Peroxynitrite (ONOO$^-$) reacts with tyrosine residues to yield 3-nitrotyrosine (3-NT), a stable marker of ONOO$^-$ formation (6). We measured free and protein-bound 3-NT in BALF by HPLC with electrochemical detection (15). Protein was precipitated from BALF with ethanol and then hydrolyzed with pronase, after which 3-NT was assayed using HPLC with a Shimadzu solvent delivery system (model 580; ESA, Chelmsford, MA) and a reversed-phase C18 column (5-µm bead size; 4.6 × 150 mm; mobile crystalline material). Isocratic elution was performed using a mobile phase of 50 mM acetic acid, 50% sodium hydroxide, and 15% methanol (pH 4.7). For the dual-channel electrochemical detector (Coulochem II, ESA), the potential for channel A was poised at +600 mV to quantify tyrosine and aminotyrosine as well as remove compounds oxidized at lower potentials (54). Channel B, downstream of channel A, was set to +800 mV to detect 3-NT. This arrangement optimizes detection of 3-NT in samples containing significant amounts of tyrosine. The retention time for 3-NT was 7 min longer than for tyrosine, allowing a 1,000-fold enhancement of sensitivity to 3-NT by programming a variable gain into the detector. A guard cell set to +850 mV was interposed between the solvent delivery system and injector to remove electrochemically active compounds from the mobile phase. The retention time for 3-NT was confirmed by using authentic standards and by addition of 10 mM sodium hydrosulfite (dithionite) to 3-NT, resulting in reduction to aminotyrosine and changes in retention time and electrochemical characteristics. Data were expressed as 3-NT content in 20 µl of sample.

Assessment of CNS toxicity. All experimental animals were continuously visually monitored throughout all hyperoxic exposures for evidence of CNS toxicity. Signs included restlessness, rigidity, excessive cleaning movements, salivation, shaking, deep breathing movements, and convulsions.
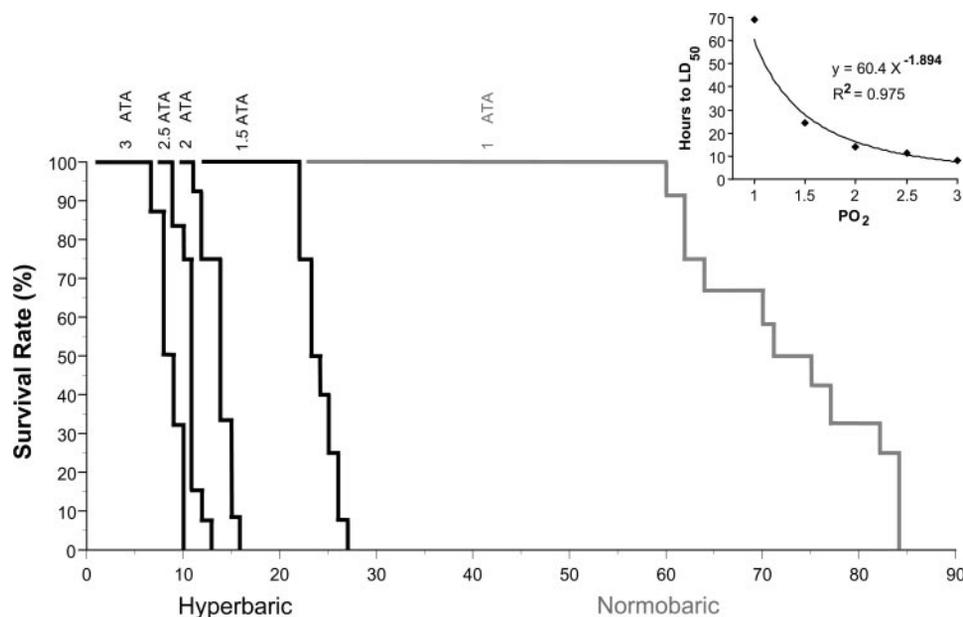
Fig. 1. Survival analysis. Age-matched, freely moving rats were exposed to normobaric hyperoxia [>98% O_2 at 1 atmosphere absolute (ATA)] or hyperbaric hyperoxia (>99% O_2 at 1.5, 2.0, 2.5, and 3.0 ATA). Survival rate vs. time was plotted for each exposure ($n = 10$–12, each group). *Inset*: as inspired P_{O_2} increases, exposure time required for 50% mortality (LD_{50}) decreases exponentially.

Arterial blood gases and pH. Samples of arterial blood were drawn from the abdominal aorta, or from a femoral artery, before lung lavage, and blood gases and pH were measured with a blood gas/pH analyzer (model 1304; Instrumentation Laboratory, Lexington, MA).

Vagotomy. In one group of rats ($n = 13$), the left vagus nerve was transected at the cervical level. Using sterile procedure, an incision was made in the neck, and the vagus was carefully exposed by blunt dissection. The nerve was cut in two places so that a 1-mm section could be removed, and the wound was closed and sutured. Each of these animals was allowed to recover for 1 wk before exposure to hyperoxia. From eight of these animals, BALF was withdrawn from both lungs. In the remaining five animals, the

contralateral bronchus was clamped to permit selective BAL of only the ipsilateral lung.

Statistical analysis. All values are expressed as means ± SE unless otherwise stated. Statistical evaluations were performed with commercially available software (Statview, Calabasas, CA) using one-way ANOVA and Scheffé's post hoc test. A P value of <0.05 was considered significant.

RESULTS

Animal survival in hyperoxia. Figure 1 shows survival curves for rats exposed to normobaric O_2 (1 ATA) or hyper-
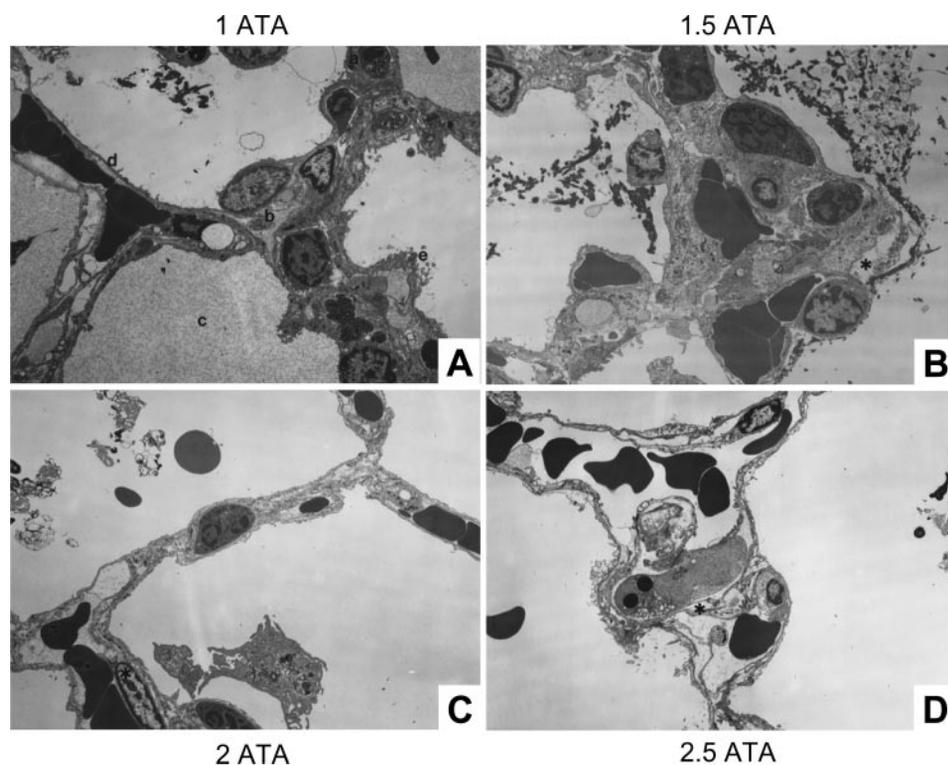

Fig. 2. Pathology. Representative electron micrographs of rat lungs are shown from 4 levels of hyperoxia (magnification ×6,800). *A*: in 1 ATA O_2, lethal lung injury occurred between 60–80 h, characterized by damage to capillary endothelium and alveolar epithelium, an increase in inflammatory cells in the interstitium ("a"), as well as edema in the interstitium ("b") and in the alveoli ("c"). Note the separation of endothelium from basement membrane ("d") and the ruffling of type I alveolar cell membranes ("e"). *B*: in 1.5 ATA O_2, patterns of injury to endothelial and epithelial cells are comparable with those seen at 1 ATA. Note interstitial edema at *. *C*: in 2.0 ATA O_2, lung injury is lethal at a mean time of 14 h. Again, epithelial cell membranes are ruffled, and capillary endothelium is lifted from underlying basement membrane. Unlike exposures at 1 or 1.5 ATA, however, neither interstitial nor alveolar edema is prominent here. Clumping and margination now appear in endothelial cell nuclear chromatin (*). *D*: in 2.5 ATA O_2, central nervous system toxicity was manifested in this animal, which resulted in more severe endothelial and epithelial injury, with some areas of alveolar septae almost completely denuded of type I epithelium (*). There is no infiltration of inflammatory cells, but endothelial cells are markedly swollen, and capillary lumina are packed with red blood cells to a greater extent than seen at the other exposures.

baric O$_2$ (1.5, 2, 2.5, and 3 ATA). The LD$_{50}$ decreased exponentially as inspired P$_{O_2}$ increased, approximating the curve LD$_{50}$ = 60 (P$_{O_2}$)$^{-1.9}$, R^2 = 0.975 (Fig. 1, *inset*). In normobaric hyperoxia, LD$_{50}$ occurred at ~69 h. In hyperbaric hyperoxia, LD$_{50}$ dropped to 24.2 h at 1.5 ATA, 14.2 h at 2.0 ATA, 11.2 h at 2.5 ATA, and 8.3 h at 3.0 ATA. Shorter exposure times (~80% of LD$_{50}$) were chosen for the remaining experiments: 56 h for 1 ATA, 20 h for 1.5 ATA, 10 h for 2 ATA, 8 h for 2.5, and 6 h for 3 ATA.

Animal behavior in hyperoxia. All rats exposed to 1 ATA O$_2$ for 56 h survived with no sign of seizures. Similarly, rats exposed to O$_2$ at 1.5 ATA for 20 h or at 2 ATA for 10 h showed motor impairment but no excitability or seizures. At 2.5 ATA, 2 of 14 (14%) animals convulsed during the 8-h exposure, and at 3 ATA, 6 of 16 animals (37%) did so between 4–6 h. Most rats exposed to O$_2$ at 3 ATA exhibited spasticity, rigidity, and kangaroo-like posturing, and two animals showed forelimb paresis.

Gross and microscopic pathology of the lung. After 56 h at 1 ATA O$_2$, lungs were grossly edematous and congested, and diffuse pulmonary hemorrhage was observed in some animals. Light microscopy disclosed accumulations of inflammatory cells in interstitial and alveolar spaces. Qualitative surveys of the electron micrographs typically revealed damage to capillary endothelium and alveolar epithelium, an increase in interstitial cells, and interstitial and alveolar edema (Fig. 2*A*). Endothelial injury was the most striking feature, with pyknotic nuclei and swelling of perinuclear cisternae, rough endoplasmatic reticula, and mitochondria. There was localized destruction of endothelial cell membranes, and some cells were lifted off the basement membrane. Capillary lumina were packed with red blood cells and platelets. Damage to epithelial cells was less prominent, consisting of a ruffling of type I cell membranes and a blunting of type II cell microvilli. Although damage was considerable, a few areas appeared to be relatively normal.

For rats exposed to 1.5 ATA O$_2$ for 20 h, changes seen on the electron micrographs were similar to those seen at 1 ATA with only quantitative differences. Thus endothelial cell separation from the basement membrane tended to be more widespread, there was more edema in type I epithelium (Fig. 2*B*), but far fewer inflammatory cells had accumulated within the interstitium. It was after exposure to higher pressures that qualitative differences began to appear. Therefore, following 10 h at 2.0 ATA O$_2$, nuclei of endothelial cells were now affected, manifested by clumping and margination of chromatin; this was in addition to further separation of endothelial cells from basement membrane (Fig. 2*C*). Overall, the damage became even less inflammatory in character, with reduced thickening of alveolar septa, decreased interstitial edema, and fewer inflammatory cells. In contrast to the injury pattern seen at 1 or 1.5 ATA, no areas of epithelium were unaffected. Because the patterns of injury seen at 1 and 1.5 ATA O$_2$ were similar, with important differences only appearing at 2 ATA and above, we omitted studies of some markers of pulmonary injury at 1.5 ATA.

Rats exposed to O$_2$ at 2.5 ATA for 8 h showed even more severe damage to type I epithelial cells, which in some places had sloughed off into the alveolar space, denuding the basement membrane (Fig. 2*D*). The interstitium was edematous, although with no abnormal increase in cellularity, and endo-

thelial cells were markedly swollen. Capillary lumina were engorged with red blood cells to a greater extent than at any other exposure levels.

Lung-injury scores (Fig. 3) derived from semiquantitative analysis of light micrographs reveal that all three indices of pulmonary injury show an initial peak after 56 h at 1 ATA and progressively diminish as P$_{O_2}$ is increased to 1.5 and then to 2 ATA. Compared with 1 ATA, alveolar debris is decreased sevenfold at 2 ATA, and alveolar edema is essentially undetectable. At 2.5 ATA, this trend is reversed: all three components of injury are now at least as great as after the much longer 1 ATA exposure. Multiple sections of inflation-fixed lungs from rats exposed to hyperbaric normoxia (7% O$_2$, balance N$_2$) at 3 ATA for 6 h showed neither gross abnormalities nor significant pathology by light microscopy (data not shown).

Pleural fluid volume and lung edema. During normobaric hyperoxia, pleural fluid volume increased progressively with duration of exposure, from 0.4 ± 0.07 ml after 24 h to 10.8 ± 1.8 ml after 56 h (Fig. 4). However, of the four levels of hyperbaric exposure studied, only 1.5 ATA produced significant accumulations of pleural fluid during the 20-h exposure, comparable to that produced at 1 ATA after 48 h.

Wet-dry ratio, an indicator of pulmonary edema, increased with duration of normobaric exposure to O$_2$ and, after 56 h, reached a maximum of 6.3, ~1.3× that in air-breathing controls (Fig. 4). For the HBO$_2$ exposures, wet-dry ratio increased significantly (with respect to air breathing controls) only at 1.5 ATA O$_2$.
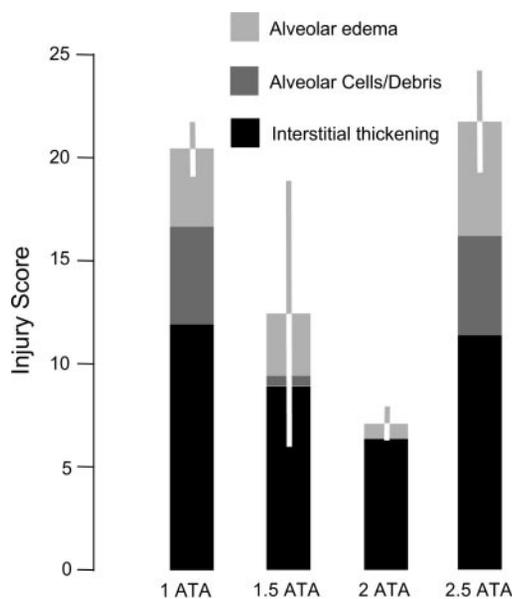

Fig. 3. Lung injury scores. Three indices of lung injury derived from semiquantitative analysis of light micrographs were combined to produce a comprehensive measure of hyperoxic damage (n = 6 for each level of hyperoxia). Black segments indicate interstitial thickening. Medium gray segments indicate the presence of intra-alveolar cells and debris, including both inflammatory and noninflammatory cells as well as cell components. Light gray segments show fluid in alveoli, which correlates with edema. All 3 indices show an initial peak after 56 h at 1 ATA and progressively diminish as P$_{O_2}$ is increased to 1.5 and then 2 ATA. Compared with 1 ATA, alveolar debris is decreased 7-fold at 2 ATA, and alveolar edema becomes undetectable. This downward trend is reversed at 2.5 ATA after 8 h: all 3 components of injury are now as great as after the much longer 1 ATA exposure.
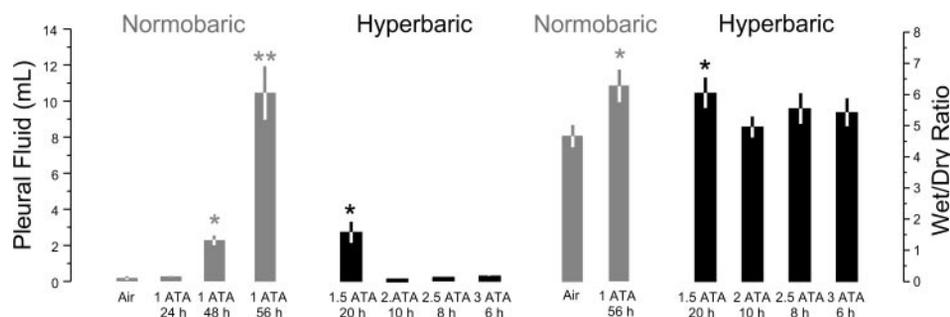
Fig. 4. Pleural fluid and wet-dry ratio. *Left*: pleural fluid was measured in rats immediately before lung lavage. Mean volume ± SE of pleural fluid for each hyperoxic exposure ($n = 8–10$, each group) was compared with that taken from control animals breathing room air (*$P < 0.05$ vs. air breathing; **$P < 0.01$). *Right*: mean lung wet-dry ratio ± SE, as an index of edema, was assessed in all groups of rats exposed to normobaric and hyperbaric oxygen and was compared with ratios from lungs of control animals breathing room air (*$P < 0.05$ vs. air).

Lung inflammation and injury. After 48–56 h of normobaric O$_2$, total inflammatory cell counts in BALF were significantly above control levels (Fig. 5). Rats exposed to 2.5 and 3 ATA O$_2$ also had significantly increased BALF cell counts compared with air controls but much lower than after normobaric exposure. BALF LDH increased progressively during normobaric O$_2$ exposure and, after 56 h, was 7.5-fold higher than during air breathing (Fig. 5). LDH activity in rats exposed to HBO$_2$ also increased significantly compared with air-breathing controls but with no statistically significant differences among those exposed to 2.0, 2.5, and 3.0 ATA O$_2$ (Fig. 6). Total protein concentration in BALF also increased in a time-dependent manner in normobaric hyperoxia. At 2.5 and 3 ATA (but not at 2 ATA), BALF protein was significantly higher than in air controls and notably different from the pattern for BALF LDH, suggesting that a separate mechanism contributes to transepithelial protein leak in hyperbaric hyperoxia above 2 ATA O$_2$.

Blood gases. Hyperbaric oxygen exposures at 1.5 ATA (20 h, $n = 8$) and 2.0 ATA (10 h, $n = 11$) produced a characteristic hyperoxic hyperventilatory response (17) with significant decreases in Pa$_{CO_2}$ and increases in arterial pH compared with respective 0-h control values (all $P < 0.05$). The ratio of arterial Po$_2$ to alveolar Po$_2$ (arterial-alveolar ratio) decreased in animals after 20 h at 1.5 ATA O$_2$ ($0.62 ± 0.07$ vs. $0.74 ± 0.05$; $P < 0.01$) but not in animals exposed to 2.0 ATA O$_2$ for 10 h. In contrast, animals breathing O$_2$ at 3.0 ATA did not demonstrate either hyperventilation or a change in arterial-alveolar ratio by the end of the 6-h exposure compared with room-air controls.

Changes in NO$_x$ and 3-NT. Oxygen at 1 ATA increased NO$_x$ in BALF progressively over 56 h of exposure. After 48 h, total NO$_x$ had increased significantly, and after 56 h, it had risen sevenfold over that of air-breathing controls (Fig. 7). At 3 ATA, NO$_x$ levels in BALF were higher than in air-breathing controls but significantly less ($P < 0.05$) than was seen after 56 h of normobaric hyperoxia. BALF 3-NT was below the limit of detection (0.1 pM/20 μl) in control rats breathing air but was readily measured in rats breathing normobaric oxygen

for 24 h, and it progressively increased with longer exposures (Fig. 7). Rats exposed to 3 ATA also showed increased 3-NT but less than in rats under normobaric hyperoxia for 56 h.

Lung injury in rats with convulsions. Rats exposed to 3 ATA for 6 h ($n = 37$) were divided into two groups based on the presence ($n = 14$) or absence ($n = 23$) of convulsions, and their lung injury endpoints were compared. Significant differences in wet-dry ratio as well as in BALF LDH and total protein content were observed between the two groups. The occurrence of convulsions correlated with a greater severity of acute edema, cellular damage, and disruption of the blood-alveolar barrier (Fig. 8).

NOS inhibition and lung injury. To evaluate the contribution of NO to lung injury, rats were treated with either the nonspecific NOS inhibitor, L-NAME, or the nNOS inhibitor, 7-NI. Either of these agents provided some protection to the lung from cell damage and protein leakage (Fig. 8).

Effects of vagotomy on lung injury. When unilateral, cervical vagotomy was performed 1 wk before exposure to 3 ATA O$_2$, hyperoxic pulmonary injury was diminished. Analysis of BALF from these animals showed that total protein and LDH were ~60% and 45%, respectively, of the values seen in animals without vagotomy (Fig. 9). Concentrations of BALF protein and LDH in the ipsilateral lung were below the corresponding aggregate values from both lungs, but only the protein data reached statistical significance.

DISCUSSION

Our results clearly demonstrate three novel points, which together provide a new perspective on the etiology of pulmonary injury in hyperbaric hyperoxia. First, oxygen exposures at hyperbaric levels that induce CNS toxicity are accompanied by a different pattern of lung histopathology than that seen in normobaric hyperoxia, and thus rats exposed to hyperbaric oxygen were most likely to manifest this pattern of pulmonary injury if they had also exhibited convulsions. Second, this
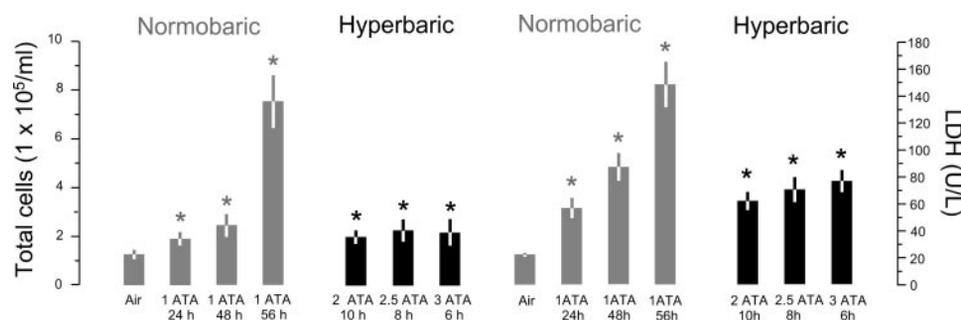

Fig. 5. Inflammatory cells and lactate dehydrogenase (LDH) in bronchoalveolar lavage fluid (BALF). *Left*: macrophages, eosinophils, and neutrophils were counted in BALF withdrawn from rats after exposure to normobaric or hyperbaric oxygen. Values are means ± SE ($n = 8–12$, each group) of total cells in 1-ml samples. Results are compared with values from control animals breathing room air (*$P < 0.05$ compared with air). *Right*: catalytic activity of LDH (U/l) was measured in cell-free BALF. Values are means ± SE ($n = 10–12$, each group) for animals exposed to hyperoxia (*$P < 0.05$ compared with air).
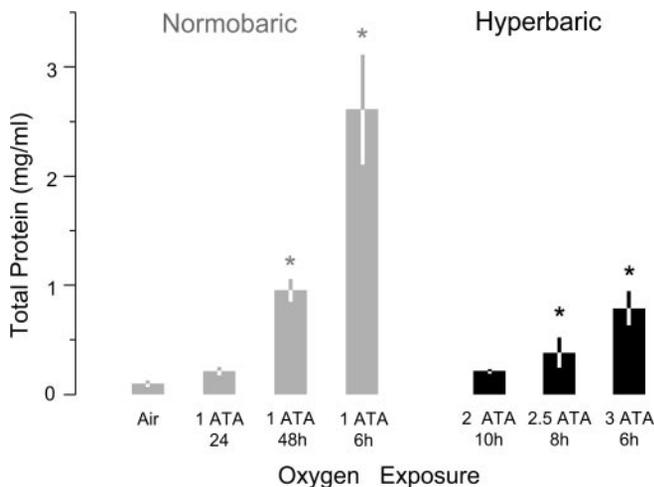
Fig. 6. Protein infiltration. Values are means ± SE ($n = 10$–12, each group) total protein (mg/ml) in BALF from rats exposed to 5 levels of hyperoxia (*$P < 0.05$ compared with air).

pattern of injury is potentiated by NO derived predominately from nNOS. Finally, this injury requires intact autonomic innervation between lung and brain since unilateral transection of the vagus nerve at the cervical level mitigated the pulmonary injury.

Although the absolute values of indices of pulmonary injury seen at 2 ATA and above were significantly less than seen at 1 ATA after 56 h, the rates at which these signs appear are clearly increased in hyperbaric hyperoxia. Also, NO$_x$ levels after 6 h at 3 ATA were about twice those in air-breathing controls and approximated those found in rats exposed to 1 ATA O₂ for 24 or 48 h, despite the much shorter exposure. The same is true for both inflammatory cells and LDH in BALF. Therefore, the underlying pathological processes in normobaric hyperoxia are accelerated by HBO₂, additional processes must come into play, or both.

The idea that lung pathology in hyperoxia may be related to sympathetic excitation is supported by several early investigations, and endogenous epinephrine was among the agents implicated (4, 33, 34). Morphological changes in the lungs of animals exhibiting convulsions or seizures in hyperbaric oxygen have also been described (2, 36), but changes in pulmonary inflammation and biochemistry were not assessed. In addition, pulmonary edema and congestion have been reported in ani-
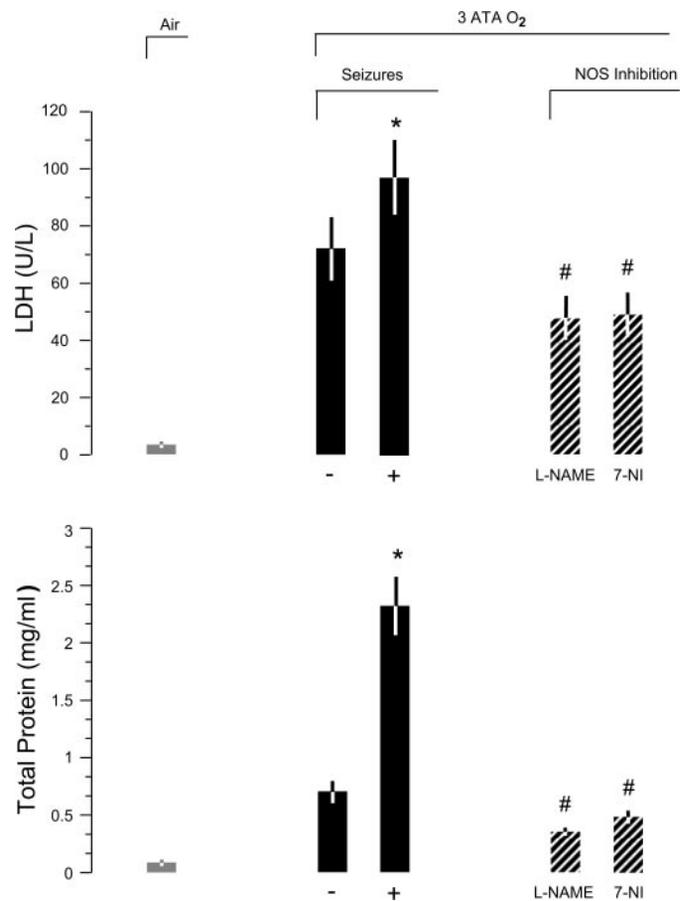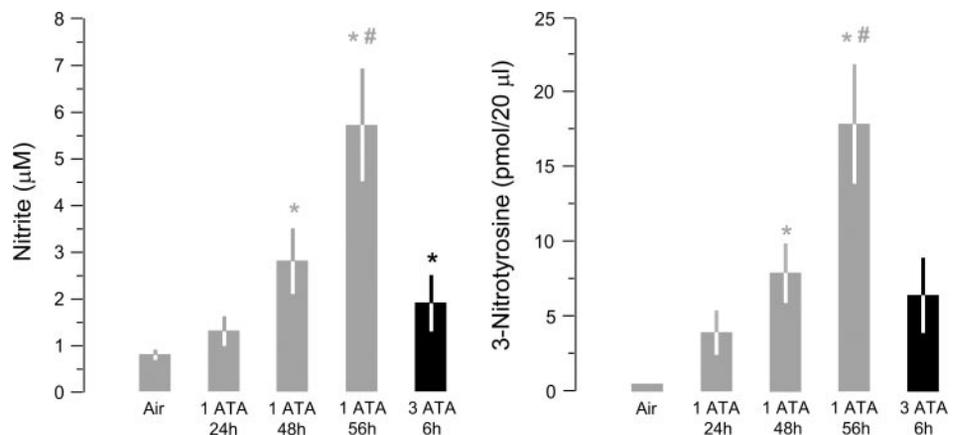

Fig. 8. Convulsions and nitric oxide synthase (NOS) inhibition at 3 ATA. *Left*: LDH and total protein in BALF from rats exhibiting convulsions were compared with values from animals not showing convulsions; air controls are shown for reference (*far left*). Both hyperoxic groups were exposed to O₂ at 3 ATA for 6 h. Results are means ± SE (*$P < 0.05$ between the 2 oxygen-exposed groups). *Right*: total protein (mg/ml) and LDH (U/l) were measured in BALF of rats exposed for 6 h to O₂ at 3 ATA after treatment with the nonselective NOS inhibitor L-NAME or the selective neuronal NOS inhibitor 7-nitroindazole (7-NI; $n = 10$–12, each group). Values are means ± SE (#$P < 0.05$ vs. untreated controls).

mals subsequent to seizures induced by hyperbaric oxygen, and those changes were prevented when seizures were inhibited, for example, by barbiturates or by GABA (5, 31, 60). Moreover, direct correlation between the numbers of repeated con-

Fig. 7. NO and ONOO⁻ production. Nitric oxide metabolites in BALF after hyperoxic exposure are expressed as means ± SE ($n = 8$–10, each group). *Left*: nitric oxide, determined as the NO metabolites NO$_2^-$ and NO$_3^-$ in BALF (*$P < 0.05$ vs. air; #$P < 0.05$ vs. 3 ATA O₂, 6 h). *Right*: peroxynitrite, determined as pmol/20 µl of BALF of 3-nitrotyrosine (*$P < 0.05$ vs. 1 ATA, 24 h; #$P < 0.05$ vs. 3 ATA O₂, 6 h).
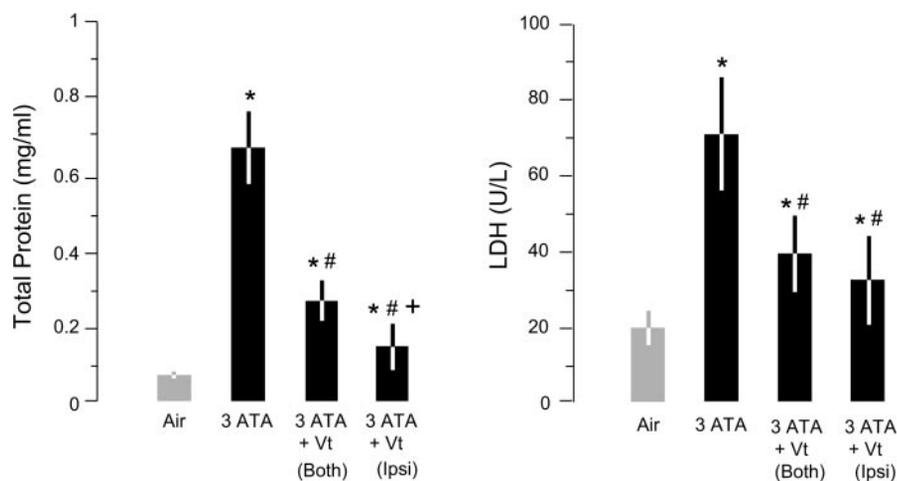
Fig. 9. Lung damage with and without vagotomy. Total protein (mg/ml) and LDH were determined in BALF of intact and vagotomized rats exposed to 3 ATA O$_2$ for 6 h ($n = 8–10$, each group). Values for BALF protein and LDH in the ipsilateral lung (Ipsi) are less than the aggregate values from both lungs (Both), but only the protein data are statistically significant. Values are means $\pm$ SE ($*P < 0.05$ vs. air; #$P < 0.05$ vs. rats without vagotomies exposed to 3 ATA; +$P < 0.05$ vs. aggregate values from both lungs).

vulsions suffered by rats and the severity of lung damage, both gross and microscopic, has also been reported (47). Thus, although circumstantial evidence has pointed to CNS mediation of hyperbaric oxygen lung injury, no mechanism has ever been elucidated.

It was shown very early that pressure per se is not likely to be a significant factor in the pulmonary toxicity of hyperbaric hyperoxia. In an elegant experiment described by Penrod in 1958 (48), the bronchi of cats were separately catheterized, and oxygen was supplied to one lung and inert gas, not air, to the other during exposure to 5 ATA for 7 h. The lung supplied with inert gas was unchanged, while the lung exposed to oxygen showed "considerable gross and microscopic damage" (48). The primary and secondary effects of pressure on pulmonary injury have also been examined in other ways as well. For example, the question of whether lung damage in hyperbaric oxygen could be caused or exacerbated by the increased density of the breathing gas was studied by Bergø and Tyssebotn in 1991 (7). These investigators reported that no significant change in pulmonary blood flow occurred in rats breathing normoxic gas at $5\times$ the density of air (7).

The prevailing view has been that normobaric and hyperbaric hyperoxia damage the lungs by the same mechanism: production of ROS or RNS. And because the rate of production of reactive species is more intense under hyperbaric conditions, damage is accelerated. There is compelling evidence from normobaric studies that ROS, RNS, and various cytokines produced in the lung induce cellular damage by oxidation of proteins, peroxidation of membrane lipids, and breakage of DNA strands (29, 30, 38, 49, 53). There is also evidence that NO specifically plays a role in the development of pulmonary toxicity induced by normobaric oxygen (1, 16, 56, 57). Although other studies have investigated changes in NO activity in brain during hyperbaric exposure to oxygen, this work is the first to evaluate RNS production in the lung under such conditions.

It remains an open question as to what extent RNS are agents of pulmonary injury in hyperoxia at 1 ATA. We did not use NOS inhibitors under normobaric conditions for both a technical and a physiological reason. Because the half-life of the inhibitors is far shorter than the hyperoxic exposures, multiple doses would have to be administered, for example by mixing inhibitors with drinking water (50), which introduces an un-

controllable variable. Also, NOS inhibition of more than a few hours creates a shifting physiological state (for example by varying kidney and cardiac function) that does not reach equilibrium for weeks (50). It would be difficult to interpret data from such an experiment. It may be possible to circumvent this problem in future studies by using NOS-knockout mice.

Overall, our findings are difficult to reconcile with the idea that the pathological processes in normobaric and hyperbaric pulmonary injury are the same. Rats exposed to 2.5 or 3 ATA without seizures show a pattern of lung damage different form that seen at 1 ATA, whereas the injury pattern in rats with seizures had similarities to those of rats exposed across the entire range of O$_2$ pressures. The most notable difference in the lung injuries at O$_2$ exposures of 2 ATA or above was the lack of inflammatory cells in BALF and lung tissue. In addition, only minor increases were found in BALF NO or ONOO$^-$ in rats exposed to O$_2$ at 3 ATA, much less than after 56 h of normobaric oxygen (see Fig. 7). Despite this, composite lung injury scores were the same after 8 h at 2.5 ATA as after 56 h at 1 ATA. This was due in part to a shift in the character of intra-alveolar cell debris seen after exposure to the higher pressure. Although far fewer intact inflammatory cells are found in BALF after 2.5 ATA compared with 1 ATA (Fig. 3), the light micrographs indicate that the total amount of intra-alveolar debris is at least as great at 2.5 ATA, consistent with more epithelial cell damage as well as with the presence of broken cell components and proteinaceous exudates after this insult.

Systemic inhibition of NOS protected against hyperbaric lung injury and prevented seizures, suggesting a relationship between the development of CNS and pulmonary O$_2$ toxicity. Moreover, the effects of nonselective (L-NAME) or selective (7-NI) NOS inhibitors on pulmonary oxygen toxicity did not differ significantly. These findings implicate NO in acute lung injury and suggest that nNOS plays the prevalent role in the development of pulmonary toxicity at 3 ATA O$_2$. This new finding is consistent with our previous work demonstrating principal role for endothelial NOS (eNOS)-derived NO in altering cerebral blood flow before CNS O$_2$ toxicity and for nNOS-derived NO in accelerating oxygen seizures through amplification of the imbalance of excitatory-to-inhibitory neurotransmission in the brain (22, 23). Although we found increases in NO$_x$ and OONO$^-$ in BALF after 56 h at 1 ATA O$_2$,

it seems unlikely that suppression of NO production in the lung at 3 ATA accounts for the protective effects of selective inhibition of nNOS. This accords with the high lung injury scores in hyperbaric exposures, even though markers for RNS in the corresponding BALF samples were quite low. It is likely that the source of NO that potentiates pulmonary injury in normobaric conditions (and appears in BALF) is different from that responsible for the distinct character of hyperbaric pulmonary injury.

Because nNOS is expressed in lung, vasculature, muscle, and elsewhere, not just in neuronal tissue, specific inhibition of this NOS isoform does not establish an exclusive connection with the CNS. However, Vaughan et al. (59) have shown that "virtually all exhaled NO in the rabbit lung is produced by eNOS, which is present throughout the airways, alveoli, and vessels." Therefore, the conspicuous effect we observed after selective inhibition of nNOS probably involves significant extrapulmonary sources of NO. Our findings, that seizures potentiate pulmonary injury and that vagotomy attenuates it, provide additional, strong evidence for CNS involvement. However, these findings, although striking, may not be unique to hyperbaric hyperoxia.

Our observation that vagotomy prevented the pulmonary injury characteristic of hyperbaric hypoxia implicates a signal from the brain in the development of this pathology. The mechanisms or possible modes of lung injury could involve NO-mediated neuronal pathways and CNS-driven central hemodynamic alterations. Work by Grandpierre and colleagues in 1957 (27) has shown that vagal transection also mitigates pulmonary injury in normobaric hyperoxia. Therefore, we do not exclude the possibility that events in the brain have a role in oxygen-induced lung injury in both normobaric and hyperbaric conditions. But the facts that the histopathologies are distinct and that seizures result in more severe pulmonary damage support our hypothesis that the CNS plays a more important role in pulmonary damage in hyperbaric hyperoxia.

The biphasic response to increasing levels of hyperoxia shown by the composite scores of lung injury (Fig. 3) suggests that at least two pathological processes are at work. The first involves time-dependent effects that are less fully developed as the duration of hyperoxic exposure decreases from 1 to 1.5 to 2 ATA. The second process supervenes as the oxygen pressure increases, for instance at 2.5 ATA, the lowest level of hyperoxia at which convulsions from CNS toxicity were observed.

Although the specific mechanisms by which neuronal NO causes lung injury in hyperbaric hyperoxia were not evaluated in the present study, the data imply that NO modulation of CNS-mediated adrenergic/cholinergic pathways leads to lung injury. Lung innervation is complex and includes not only autonomic adrenergic and cholinergic fibers, but also nonadrenergic noncholinergic (NANC) systems, which perform defensive, regulatory, and immunomodulary functions (35, 40–42, 46, 52). In the brain, the inhibitory NANC system involving NO opposes cerebral vasoconstriction (58), but in the lung, nNOS does not seem to be important for normal function, since nNOS knockout mice have normal endothelium-dependent vasodilation (24).

Although epinephrine and acetylcholine are the major neurotransmitters involved in regulating pulmonary airway and vascular function, NANC neurotransmitters, including vasoactive intestinal peptide (VIP) and NO, also appear to be important. Immunohistochemical studies have shown the existence of nNOS in nerve terminals supplying lung vessels and lower airways (25, 39). A fruitful area for further study could be the role of CNS-mediated cardiovascular contributions to lung damage in hyperbaric hyperoxia. In addition to its effects on the lung and brain, hyperbaric oxygen also increases systemic vascular resistance and reduces cardiac output. These effects could shift systemic blood to the pulmonary circulation, increasing pulmonary blood volume and pulmonary arterial or venous pressure. Although such hemodynamic alterations may be rapid and transient, structural disruption of pulmonary capillaries could cause protein-rich pulmonary edema and persistent damage to the blood-gas barrier.

In summary, we have demonstrated that as hyperoxia increases from normobaric to hyperbaric levels, lung responses shift from direct inflammatory injury to CNS-mediated noninflammatory injury, and although the differences between normobaric and hyperbaric oxygen toxicity are qualitative and not absolute, the direct effect of oxygen on the lung predominates in normobaric hyperoxia, whereas CNS effects prevail in hyperbaric conditions. As the balance between these two mechanisms shifts, the pattern of injury changes, but there is never a condition in which one or the other effect is totally lacking. The former develops slowly, and because the entire surface of the lung is directly exposed to the hyperoxic environment for many hours, the inflammatory response is diffuse with destruction of the alveolar-capillary barrier, edema, impaired gas exchange, respiratory failure, and death. However, at hyperbaric exposures, pulmonary damage develops more rapidly and is presaged by events in the brain. This more acute injury is driven by extrapulmonary mechanisms in which NO derived from nNOS may link elevated P_{O_2} in brain to accelerated damage in the lung via central autonomic pathways.

REFERENCES

1. **Arkovitz M, Szabo C, Garcia V, Wong H, Wispe J.** Differential effects of hyperoxia on the inducible and constitutive isoforms of nitric oxide synthase in the lung. *Shock* 5: 345–350, 1997.
2. **Balentine JD.** *Pathology of Oxygen Toxicity.* New York: Academic Press, 1982.
3. **Bean JW.** Effects of oxygen at increased pressure. *Physiol Rev* 25: 1–147, 1945.
4. **Bean JW, Johnson PC.** Epinephrine and neurogenic factors in the pulmonary edema and CNS reactions induced by O₂ at high pressure. *Am J Physiol* 180: 438–444, 1955.
5. **Bean JW, Zee D, Thom B.** Pulmonary changes with convulsions induced by drugs and oxygen at high pressure. *J Appl Physiol* 21: 865–872, 1966.
6. **Beckman JS, Koppenol WH.** Nitric oxide, superoxide, and peroxynitrite: the good, the bad, and ugly. *Am J Physiol Cell Physiol* 271: C1424–C1437, 1996.
7. **Bergø GW, Tyssebotn I.** Respiratory frequency and distribution of cardiac output in rats breathing gas with different densities. *Scand J Clin Lab Invest* 51: 59–56, 1991.
8. **Bitterman N, Bitterman H.** L-arginine-NO pathway and CNS oxygen toxicity. *J Appl Physiol* 84: 1633–1638, 1998.
9. **Chavko M, Xing GQ, Keyser DO.** Increased sensitivity to seizures in repeated exposures to hyperbaric oxygen: role of NOS activation. *Brain Res* 900: 227–233, 2001.

10. **Clark JM, Lambertsen CJ.** Pulmonary oxygen toxicity: a review. *Pharmacol Rev* 23: 37–133, 1971.

11. **Clark JM, Thom SR.** Oxygen under pressure. In: *Bennett and Elliott's Physiology and Medicine of Diving*, edited by Brubakk AO and Newman TS. Flagstaff, AZ: Best Publishing, 2003.

12. **Crapo JD.** Morphologic changes in pulmonary oxygen toxicity. *Annu Rev Physiol* 48: 721–731, 1986.

13. **Crapo JD.** Pathologic changes in the lungs of oxygen-adapted rats: a morphometric analysis. *Lab Invest* 39: 640–653, 1978.

14. **Crapo JD, Barry BE, Foscue HA, Shelburne J.** Structural and biochemical changes in rat lungs occurring during exposures to lethal and adaptive doses of oxygen. *Am Rev Respir Dis* 122: 123–143, 1980.

15. **Crow JP, Packer L.** Measurement and significance of free and protein-bound 3-nitrotyrosine, 3-chlorotyrosine, and free 3-nitro-4-hydroxyphenylacetic acid in biologic samples: a high-performance liquid chromatography method using electrochemical detection. In: *Methods in Enzymology*. New York: Academic Press, 1999, p. 151–160.

16. **Cucchiaro G, Tatum AH, Brown MC, Camporesi EM, Daucher JW, Hakim TS.** Inducible nitric oxide synthase in the lung and exhaled nitric oxide after hyperoxia. *Am J Physiol Lung Cell Mol Physiol* 277: L636–L644, 1999.

17. **Dean JB, Mulkey DK, Henderson RA 3rd, Potter SJ, Putnam RW.** Hyperoxia, reactive oxygen species, and hyperventilation: oxygen sensitivity of brain stem neurons. *J Appl Physiol* 96: 784–791, 2004.

18. **Demchenko IT, Atochin DN, Boso AE, Astern J, Huang PL, Piantadosi CA.** Oxygen seizure latency and peroxynitrite formation in mice lacking neuronal or endothelial nitric oxide synthases. *Neurosci Lett* 344: 53–56, 2003.

19. **Demchenko IT, Bennett PB, Piantadosi CA.** The role of nitric oxide in hyperbaric neurotoxicity. In: *High Pressure Biology and Medicine*, edited by Bennett PB, Demchenko IT, and Marquis RE. Rochester, NY: Univ. of Rochester Press, 1998, p. 331–338.

20. **Demchenko IT, Boso AE, O'Neill TJ, Bennett PB, Piantadosi CA.** Nitric oxide and cerebral blood flow responses to hyperbaric oxygen. *J Appl Physiol* 88: 1381–1389, 2000.

21. **Demchenko IT, Boso AE, Whorton AR, Piantadosi CA.** Nitric oxide production is enhanced in rat brain before oxygen-induced convulsions. *Brain Res* 917: 253–261, 2001.

22. **Demchenko IT, Oury TD, Crapo JD, Piantadosi CA.** Regulation of the brain's vascular responses to oxygen. *Circ Res* 91: 1031–1037, 2002.

23. **Demchenko IT, Piantadosi CA.** Nitric oxide amplifies the imbalance of excitatory to inhibitory neurotransmission accelerating oxygen seizures. *Undersea Hyperb Med* 33: 169–174, 2006.

24. **Fagan KA, Tyler RC, Sato K, Fouty BW, Morris KG Jr, Huang PL, McMurtry IF, Rodman DM.** Relative contributions of endothelial, inducible, and neuronal NOS to tone in the murine pulmonary circulation. *Am J Physiol Lung Cell Mol Physiol* 277: L472–L478, 1999.

25. **Fischer A, Mundel P, Mayer B, Preissler U, Philippin B, Kummer W.** Nitric oxide synthase in guinea pig lower airway innervation. *Neurosci Lett* 149: 157–160, 1993.

26. **Freeman BA, Crapo JD.** Hyperoxia increases oxygen radical production in rat lungs and lung mitochondria. *J Biol Chem* 256: 10986–10992, 1981.

27. **Grandpierre R, Grognot P, Senelar R.** Modifications des lesions pulmonaires provoque par l'inhalation d'oxygene apres section d'un nerf pneumogastrique. *J Physiol (Paris)* 48: 564–565, 1956.

28. **Hagioka S, Takeda Y, Zhang S, Sato T, Morita K.** Effects of 7-nitroindazole and *N*-nitro-L-arginine methyl ester on changes in cerebral blood flow and nitric oxide production preceding development of hyperbaric oxygen-induced seizures in rats. *Neurosci Lett* 382: 206–210, 2005.

29. **Hesse AK, Dorger M, Kupatt C, Krombach F.** Proinflammatory role of inducible nitric oxide synthase in acute hyperoxic lung injury. *Resp Res* 5: 11–16, 2004.

30. **Horinouchi H, Wang CC, Shepherd KE, Jones R.** TNF alpha gene and protein expression in alveolar macrophages in acute and chronic hyperoxia-induced lung injury. *Am J Respir Cell Mol Biol* 14: 548–555, 1996.

31. **Jamieson D, Cass N.** CNS and pulmonary damage in anesthetized rats exposed to hyperbaric oxygen. *J Appl Physiol* 23: 235–242, 1967.

32. **Jamieson D, Chance B, Cadenas E, Boveris A.** The relation of free radical production to hyperoxia. *Annu Rev Physiol* 48: 703–719, 1986.

33. **Jamieson D, Van Den Brenk HA.** Pulmonary damage due to high pressure oxygen breathing in rats. *Aust J Exp Biol Med Sci* 40: 309–314, 1962.

34. **Johnson PC, Bean JW.** Effect of sympathetic blocking agents on the toxic Action of O₂ at high pressure. *Am J Physiol* 188: 593–598, 1957.

35. **Kakuyama M, Vallance P, Ahluwalia A.** Endothelium-dependent sensory NANC vasodilatation: involvement of ATP, CGRP and a possible NO store. *Br J Pharmacol* 123: 310–316, 1998.

36. **Kistler GS, Caldwell PRB, Weibel ER.** Development of fine structural damage to alveolar and capillary lining cells in oxygen-poisoned rat lungs. *J Cell Biol* 32: 605–628, 1967.

37. **Klein J.** Normobaric pulmonary oxygen toxicity. *Anesth Analg* 70: 195–207, 1990.

38. **Kobayashi H, Hataishi R, Mitsufuji H, Tanaka M, Jacobson M, Tomita T, Zapol WM, Jones RC.** Antiinflammatory properties of inducible nitric oxide synthase in acute hyperoxic lung injury. *Am J Respir Cell Mol Biol* 24: 390–397, 2001.

39. **Kobzik L, Bredt DS, Lowenstein CJ, Drazen J, Gaston B, Sugarbaker D, Stamler JS.** Nitric oxide synthase in human and rat lung: immunocytochemical and histochemical localization. *Am J Respir Cell Mol Biol* 9: 371–377, 1993.

40. **Kubota E, Hamasaki Y, Sata T, Saga T, Said SI.** Autonomic innervation of pulmonary-artery - evidence for a nonadrenergic noncholinergic inhibitory system. *Exp Lung Res* 14: 349–358, 1988.

41. **Liu SF, Crawley DE, Evans TW, Barnes PJ.** Endothelium-dependent nonadrenergic, noncholinergic neural relaxation in guinea pig pulmonary artery. *Pharm Exp Therapeutics* 260: 541–548, 1992.

42. **Liu SF, Crawley DE, Rohde JAL, Evans TW, Barnes PJ.** Role of nitric oxide and guanosine 3′,5′-cyclic monophosphate in mediating nonadrenergic, noncholinergic relaxation in guinea-pig pulmonary arteries. *Br J Pharmacol* 107: 861–866, 1992.

43. **Misko TP, Schilling RJ, Salvemini D, Moore WM, Currie MG.** A fluorometric assay for the measurement of nitrite in biological samples. *Anal Biochem* 214: 11–16, 1993.

44. **Nussler AK, Bruckner UB, Vogt J, Radermacher P, Cadenas E, Packer L.** Measuring end products of nitric oxide in vivo. In: *Methods in Enzymology*. New York: Academic Press, 2002, p. 75–83.

45. **Oury TD, Ho Y, Piantadosi CA, Crapo JD.** Extracellular superoxide dismutase, nitric oxide, and central nervous system O₂ toxicity. *Proc Natl Acad Sci USA* 89: 9715–9719, 1992.

46. **Park JI, Shin CY, Lee YW, Huh IH, Sohn UD.** Endothelium-dependent sensory non-adrenergic non-cholinergic vasodilatation in rat thoracic aorta: involvement of ATP and a role for NO. *J Pharm Pharmacol* 52: 409–416, 2000.

47. **Patel YJ, Gowdey CW.** Effects of single and repeated exposures to oxygen at high pressure on normal rats. *Can J Physiol Pharmacol* 42: 245–264, 1964.

48. **Penrod KE.** Lung damage by oxygen using differential catheterization (Abstract). *Fed Proc* 17: 123, 1958.

49. **Pepperl S, Dorger M, Ringel F, Kupatt C, Krombach F.** Hyperoxia upregulates the NO pathway in alveolar macrophages in vitro: role of AP-1 and NF-κB. *Am J Physiol Lung Cell Mol Physiol* 280: L905–L913, 2001.

50. **Qiu C, Muchant D, Beierwaltes WH, Racusen L, Baylis C.** Evolution of chronic nitric oxide inhibition hypertension: relationship to renal function. *Hypertension* 31: 21–26, 1998.

51. **Sato T, Takeda Y, Hagioka S, Zhang S, Hirakawa M.** Changes in nitric oxide production and cerebral blood flow before development of hyperbaric oxygen-induced seizures in rats. *Brain Res* 918: 131–140, 2001.

52. **Scott JA, Craig I, McCormack DG.** Nonadrenergic noncholinergic relaxation of human pulmonary arteries is partially mediated by nitric oxide. *Am J Respir Crit Care Med* 154: 629–632, 1996.

53. **Shea LM, Beehler C, Schwartz M, Shenkar R, Tuder R, Abraham E.** Hyperoxia activates NF-kappaB and increases TNF-alpha and IFN-gamma gene expression in mouse pulmonary lymphocytes. *J Immunol* 157: 3902–3908, 1996.

54. **Skinner DC, Herbison AE.** Effects of photoperiod on estrogen receptor, tyrosine hydroxylase, neuropeptide Y, and beta-endorphin immunoreactivity in the ewe hypothalamus. *Endocrinology* 138: 2585–2595, 1997.

55. **Smith PK, Krohn RI, Hermanson GT, Mallia AK, Gartner FH, Provenzano MD, Fujimoto EK, Goeke NM, Olson BJ, Klenk DC.** Measurement of protein using bicinchoninic acid. *Anal Biochem* 150: 76–85, 1985.

56. **Steudel W, Watanabe M, Dikranian K, Jacobson M, Jones RC.** Expression of nitric oxide synthase isoforms (NOS II and NOS III) in adult

rat lung in hyperoxic pulmonary hypertension. *Cell Tissue Res* 295: 317–329, 1999.

57. **Taylor JL, Carraway MS, Piantadosi CA.** Lung-specific induction of heme oxygenase-1 and hyperoxic lung injury. *Am J Physiol Lung Cell Mol Physiol* 274: L582–L590, 1998.

58. **Toda N, Okamura T.** The pharmacology of nitric oxide in the peripheral nervous system of blood vessels. *Pharmacol Rev* 55: 271–324, 2003.

59. **Vaughan DJ, Brogan TV, Kerr ME, Deem S, Luchtel DL, Swenson ER.** Contributions of nitric oxide synthase isozymes to exhaled nitric oxide and hypoxic pulmonary vasoconstriction in rabbit lungs. *Am J Physiol Lung Cell Mol Physiol* 284: L834–L843, 2003.

60. **Wood JD, Stacey NE, Watson WJ.** Pulmonary and central nervous system damage in rats exposed to hyperbaric oxygen and protection therefrom by gamma-aminobutyric acid. *Can J Physiol Pharmacol* 43: 405–410, 1965.

61. **Zhang J, Su Y, Oury TD, Piantadosi CA.** Cerebral amino acid, norepinephrine and nitric oxide metabolism in CNS oxygen toxicity. *Brain Res* 606: 56–62, 1993.